Trends in Biotechnology

Opinion

Bringing Microscopy-By-Sequencing into View

Alexander A. Boulgakov [ID],[1,@] Andrew D. Ellington [ID],[1,2] and Edward M. Marcotte [ID][1,3,*,@]

The spatial distribution of molecules and cells is fundamental to understanding biological systems. Traditionally, microscopies based on electromagnetic waves such as visible light have been used to localize cellular components by direct visualization. However, these techniques suffer from limitations of transmissibility and throughput. Complementary to optical approaches, biochemical techniques such as crosslinking can colocalize molecules without suffering the same limitations. However, biochemical approaches are often unable to combine individual colocalizations into a map across entire cells or tissues. Microscopy-by-sequencing techniques aim to biochemically colocalize DNA-barcoded molecules and, by tracking their thus unique identities, reconcile all colocalizations into a global spatial map. Here, we review this new field and discuss its enormous potential to answer a broad spectrum of questions.

Merging Individual Spatial Colocalizations into a Global Positional Map, without Looking

'It is very easy to answer many of these fundamental biological questions; you just *look at the thing!*', Richard P. Feynman, *There's Plenty of Room at the Bottom*, 1959 [1]

The spatial positioning of molecules and cells is fundamental to a deeper understanding of biological systems [2–6]. Traditional optical microscopy [7] and newer, higher resolution techniques [8–10] have contributed tremendously to biological knowledge. The spatial proximity of biological components has also been inferred using biochemical techniques such as yeast-two-hybrid, cofractionation or affinity purification mass spectrometry, coimmunoprecipitation, chromosome conformation capture, BioID, APEX, and others [11–19]. Such biochemical localization approaches have several advantages over microscopy: they do not rely on the transmissibility of electromagnetic waves (often achievable only by thinly slicing or otherwise specially preparing samples) and they are not constrained to a microscope's field of view, ultimately allowing higher throughput [20].

Unfortunately, biochemical approaches (other than those based on chromosomal crosslinking; see below) often suffer from the limitation that they can only capture the colocalization of two or three individual molecules. To overcome this limitation, microscopy-by-sequencing, or DNA microscopy [20] for short, is an emerging class (Box 1) of biochemical techniques that use **oligonucleotide** (see Glossary) barcodes to recover molecules' spatial positions and thereby provide a more global map of positions for a complex molecular population. (Note that chromosomal crosslinking approaches enjoy the same benefits by virtue of also using DNA barcodes: in their case the genome itself provides the barcoding information!)

All techniques of DNA microscopy conceptually follow the same series of steps (Figure 1, Key Figure). The central concept is that barcodes confer to each molecule a unique identity that can persist through various steps of physical manipulation and that such identities ultimately denote positions. To the extent that position can be encoded in sequence, then large numbers of different barcodes, or combinations of barcodes reflecting physical juxtaposition, can be read out

Highlights

DNA microscopy computationally can already recover spatial positions for thousands, potentially millions, or billions in the future, of molecules via sequencing.

DNA microscopy sidesteps some of the limitations of optical microscopy; in principle, it can spatially locate molecules across a broad range of experimental contexts.

The large extant toolbox for DNA manipulation allows for many diverse strategies and various applications.

The strengths of DNA microscopy are complementary to extant biochemical and optical localization approaches and may help break new ground in fields such as brain connectomics and developmental biology.

[1]Center for Systems and Synthetic Biology, Institute of Cellular and Molecular Biology, Department of Molecular Biosciences, University of Texas at Austin, Austin, TX 78712, USA
[2]www.ellingtonlab.org
[3]www.marcottelab.org

*Correspondence:
marcotte@icmb.utexas.edu
(E.M. Marcotte).
@Twitter: @alex_boulgakov
(A.A. Boulgakov) @CSSBatUT
(A.D. Ellington) and @edward_marcotte
(E.M. Marcotte).

using next-generation DNA sequencing (NGS). The use of barcodes and NGS in turn allows multiplexing of large numbers of different molecules or samples simultaneously, as opposed to more traditional optical methods [5]. For example, fluorescence microscopy is limited to four, perhaps five, orthogonal fluorophores and hence fewer concurrent targets.

While the commonality of barcoding and NGS unites different approaches to DNA microscopy, each scheme has its own unique flavor.

DNA Microscopy by Amplicon Diffusion

Weinstein and colleagues [20] have recently demonstrated an **amplicon** diffusion-based DNA microscopy (Figure 2A). The authors fix cells and then reverse transcribe several mRNA species of interest into **cDNAs** bearing unique molecular identifiers (UMIs) (i.e., Figure 1 step 1). **PCR** is then performed on the fixed cells, further amplifying the cDNAs with **primers** that are designed to allow two PCR products that encounter each other via diffusion to overlap and concatenate into a single product (Figure 1 step 2). The PCR is also designed to introduce an additional unique identifier for each individual concatenation event [**unique event identifier (UEI)** [20]. Thus, as the PCR reaction progresses, products diffuse through the fixed cell, encountering each other and producing pairwise records that contain three pieces of information: the identities of the original mRNAs, their respective UMIs to distinguish each individual mRNA molecule from its peer, and UEIs to distinguish individual concatenation events produced by diffusing amplicons.

Together, this information leads to a count of how many times diffusing amplicons that arose from two different mRNAs encountered and concatenated with each other (Figure 1 step 3). The number of concatenation events has in turn been found to be related to the rate of molecular diffusion, and hence inversely to spatial distance (Figure 1 step 4). Once all overlap events are observed by deep sequencing, a diffusion-distance model can infer the relative original positions of each mRNA (Figure 1 step 5). Precision of the recovered positions is directly related to the number of overlap events sequenced: the more overlap products sequenced, the more precise the inferred positions.

One of the most important characteristics of any method to recover spatial positions is, naturally, the distance error between the recovered positions and ground truth. In the case of amplicon diffusion, Weinstein and colleagues treat their distance analysis in terms of 'diffusion distance' as the fundamental unit, with this unit's precise value dependent on the diffusion constant of the PCR products in the cells. Thus, they do not report a value for distance error in absolute units, but rather only in terms of their diffusion distance unit.

DNA Microscopy via Auto-cycling Proximity Recording (APR)

In 2017, Schaus and colleagues [21] experimentally demonstrated APR (Figure 2B), a method in which proximal pairs of DNA-barcoded **probes** interact to produce double-stranded DNA molecules containing both barcodes (i.e., Figure 1 step 2). The initial probes are specially designed oligonucleotides that must first be affixed to a surface or to molecules of interest (Figure 1 step 1). Each probe contains a primer annealing site and oligonucleotides that can bind simultaneously to two probes to create a template that can be isothermally amplified, capturing the probes' internal barcodes and thereby a double-stranded proximity record of a probe pair (Figure 1 step 2). This isothermal reaction produces many identical pairs between any two adjacent probes over the course of an experiment and these pairwise records can then be read out *en masse* by NGS (Figure 1 step 3). Alternatively, probe barcode-specific PCR amplification can be carried out to interrogate whether a particular pair of probes was adjacent or not: gel electrophoresis of all possible pairwise PCR products yields a Boolean **adjacency matrix** [22] for all probes. Either method recovers the multiple pairwise proximities

Glossary

Adjacency matrix: a matrix representing a simple graph, with each element A_{ij} set to 1 if vertices i and j are adjacent (connected) and set to 0 otherwise.

Amplicon: a double-stranded copy of a DNA template generated by PCR.

cDNA: complementary DNA synthesized from a single-stranded RNA (e.g., an mRNA).

Force-directed graph layout algorithm: an algorithm to calculate the layout of a graph using only information contained in the graph itself, modeling distances between nodes with physical forces (such as springs).

Hypergraph: a generalization of graphs where edges can join any number of vertices [46].

Ligase: an enzyme that can ligate two strands of DNA end-to-end into a single strand.

Oligonucleotide: a short strand of DNA.

PCR: polymerase chain reaction. A reaction that can create many copies of a DNA sequence from even a single template molecule.

Polony: a portmanteau of 'polymerase colony' (i.e., a patch of DNA clonally amplified into a spatial cluster).

Primer: an oligonucleotide complimentary to an RNA or DNA strand necessary for the initiation of DNA synthesis (e.g., during primer extension or PCR).

Primer extension: extending an annealed primer using a polymerase, capturing the entirety of the primer's target sequence into a complimentary strand. This is identical to the extension/ elongation step in PCR but without the complimentary primer, so as to create one-sided copies and not to yield exponential amplification.

Probe: synonym for an oligonucleotide that is used to label a molecule or a spatial position.

Restriction enzyme: an enzyme that can cut a strand of DNA, usually at a sequence-specific location.

Unique event identifier (UEI): from Weinstein *et al.*'s [20] amplicon diffusion approach; a unique barcode inserted into every pairwise amplicon concatenation event, distinguishing that individual molecular concatenation event from all others.

Voronoi tessellation: a tessellation of plane given a set of points {p_1, ... , p_k} is the set of regions completely covering

needed to reconstruct the larger graph (Figure 1 step 4); the NGS strategy is higher throughput, while the pairwise PCR interrogation is simpler for small test cases.

Note that unlike amplicon diffusion above, which for every pair of mRNAs generates many distinct barcode pairs with varying UEIs, APR makes only one pairwise adjacency record (modulo identical copies) for neighboring probes. This exemplifies an important conceptual difference between DNA microscopy strategies that must be considered in practical applications (Box 2).

As a proof-of-concept, the authors demonstrate that they can recover complex geometries as represented by probes deposited on DNA origami, whose structure ensures defined probe anchoring positions. Amplification products analyzed by gel electrophoresis yielded an adjacency matrix for all probes (Figure 1 step 4). The authors then apply a **force-directed graph layout algorithm** [23] on this adjacency matrix to recover probe positions (Figure 1 step 5), confirming the geometry defined by the original DNA origami. The errors in recovered probe positions are on the order of probe pair lengths, approximately 20–30 nm.

Puzzle Imaging (Voxel Sequencing) DNA Microscopy

In 2015, Glaser and colleagues [24] proposed and computationally explored puzzle imaging (Figure 2C), in which multiple cells are each filled with a unique per-cell DNA barcode

the plane such that each region is made of points closer to one of the points p_i than any of the others.

Voxel: the 3D analog of a 2D pixel; can be interpreted as a portmanteau of 'volume pixel'.

Box 1. A New Field Coalesces on Twitter and *bioRxiv* over the Course of Just 1 Week

The day after we uploaded our iterative proximity ligation preprint [28] to *bioRxiv* and Tweeted its arrival, we received an email from Joshua Glaser [27], also thinking about oligonucleotides and spatial positions by sequencing. Four days later, Joshua Weinstein and colleagues posted their *bioRxiv* preprint on 'DNA microscopy' [20], and 2 days after that, Ian Hoffecker and colleagues posted theirs [29]. Twitter was used throughout to share the preprints, with some representative Tweets in Figure I (there were many others!).

We were astounded. Before, we were only aware of one other paper thinking along the same lines as we were [24]. Now, in just 1 week, all groups were mutually aware of each other's ideas: a new field of research had formed. DNA microscopy was clearly an idea whose time had come.
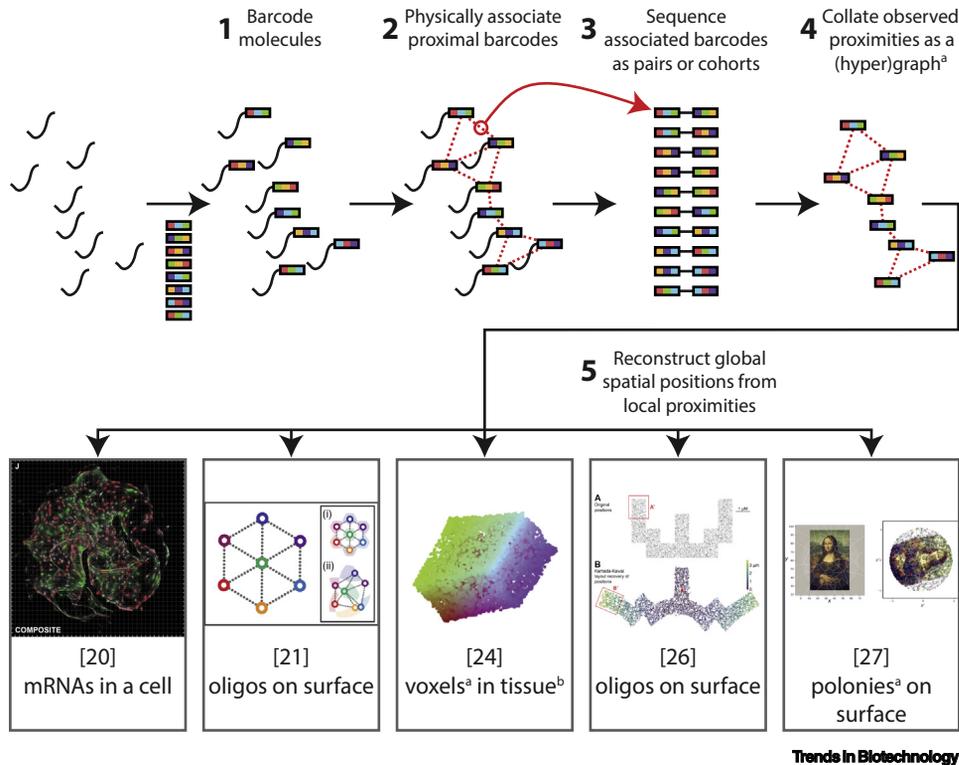

Figure I. Some of the Tweets Exchanged over a Period of Several Days as DNA Microscopy Preprints Were Uploaded.

DNA Microscopy Reconstructs Spatial Layout of DNA Molecules from Individual Proximities

Figure 1. Conceptually, the five DNA microscopy schemes reviewed herein all follow these general steps: (1) molecules of interest are barcoded with distinct DNA oligonucleotides; (2) barcodes from neighboring molecules are physically associated such that they are sequenced as one cohort, for example, as concatenated barcode pairs, with sequencing information directly reflecting their proximity (3) (see Box 2 for an important conceptual distinction in how neighboring barcodes are associated); (4) the individual proximities captured by sequencing are abstracted into a **(hyper)graph**, with nodes representing barcoded molecules and edges representing the observed proximities; (5) computational algorithms reconstruct from this graph the global map of all spatial positions. [a]See Glossary for term definitions (from [24,27,46]). [b]Glaser and colleagues also propose other variations in other contexts. Figures from original papers reused as avatars with permission. See also [20,21,26].

(i.e., Figure 1 step 1). The sample is then randomly broken up into chunks, termed **voxels** [25], with each voxel containing some mixture of barcodes by virtue of encompassing multiple cells or pieces of cells (Figure 1 step 2). All barcodes within each chunk are sequenced (Figure 1 step 3), and the physical proximity of cells is inferred if their barcodes co-occur in a single voxel (Figure 1 step 4). Multiple proximities between a cell and its neighbors can be computationally merged to recover the spatial organization of the whole (Figure 1 step 5).

The experimental contexts and methodological details simulated in this work are diverse and therefore the errors in recovered positions vary significantly between each instantiation. However, it can be generally stated that the error in voxel positions increases (in a nonlinear

(A) [20] mRNAs in a cell
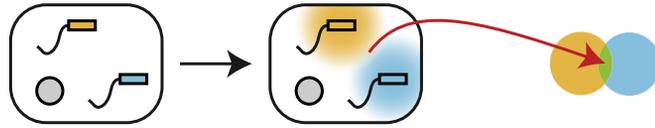
(B) [21] Oligos on surface
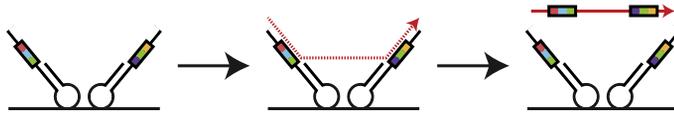
(C) [24] Voxels in tissue
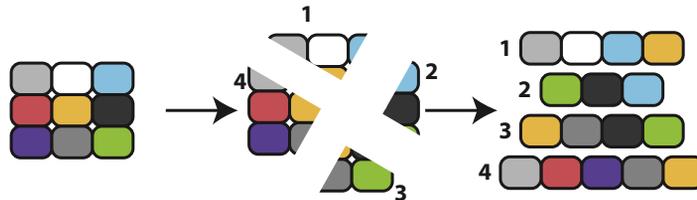
(D) [26] Oligos on surface
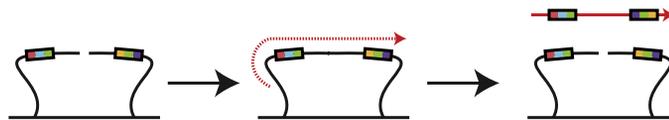
(E) [27] Polonies on surface
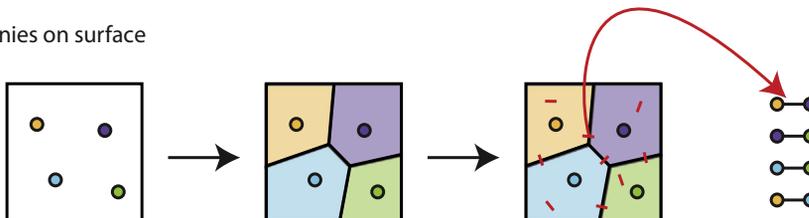
Trends in Biotechnology

Figure 2. A Variety of Methods Can Be Used to Capture Proximity Information for DNA Microscopy. (A) mRNAs in a fixed cell are barcoded during reverse transcription and then PCR amplified. As their amplicons diffuse, they concatenate with amplicons from other mRNAs, with each concatenation event also receiving its own unique barcode. The number of concatenation events between two mRNAs is inversely related to their proximity. (B) Primer extension across proximal pairs of barcoded hairpin probes captures their barcodes on a single DNA strand. (C) Cells are filled with unique per-cell barcodes. The sample is then shattered into random chunks and the barcode content of each chunk is sequenced. Barcodes sharing a chunk indicate neighboring cells. (D) Primer extension across reversibly ligated proximal pairs of barcoded probes captures their barcodes on a single DNA strand. (E) Barcoded oligonucleotides are deposited onto a surface of primers and amplified into tesselating polonies. Bridging oligonucleotides are deposited onto the polony surface and primer extended to capture identities of the molecules they bridge. Bridges across polony boundaries indicate their adjacency. See also [20,21,24,26,27].

and context-specific manner) with the size of average voxel assumed. For example, 10 μm voxels yield an average error in position of approximately 10 μm, while 2 μm voxels yield an average error of approximately 5 μm. In a simulation of pyramidal cells recovered from a rat cortex, where the

Box 2. Singleton versus Population DNA Microscopy Approaches

One of the five methods summarized above, APR [24], assigns each molecule one barcode and then records only the pairwise adjacency between those very molecules; whereas another method, amplicon diffusion DNA microscopy [20], generates multiple, distinct copies of barcodes for each original molecule and records many pairwise adjacencies between each population. Therefore, we distinguish the former type of approach as being singleton-based versus the latter as being population-based, depending on whether the barcoded molecules are amplified into a heterogeneous population or not.

Singleton approaches do not have to take into account how a replicated population of each barcoded molecule behaves; population approaches have to model replication of the barcode through space (and time) if they are to successfully infer the position of the original molecules of interest. In the amplicon diffusion approach, for example, the authors had to create and experimentally confirm models about how PCR products diffuse throughout a fixed cell as the reaction proceeds. Furthermore, we expect population approaches in general to require greater sequencing depth per label to achieve positional precision comparable with that of singleton approaches. Population approaches, however, have the advantage that they can ostensibly capture neighborhood relationships over much longer distances than singleton approaches, which are limited to capturing only pairs reachable by each (immobilized) molecule in their immediate neighborhoods.

This can also be restated as a trade-off: singleton approaches require a denser initial population of barcoded molecules and sequencing a sufficient number of their pairwise relationships; whereas population approaches can interrogate the same volume (area) with fewer labels, but require observing multiple pairwise relationships between two neighboring barcodes to precisely recover their positions.

neurons can form synapses over 200 or even 300 µm away from their center, the positional error of the neuron centroids was approximately 20–40 µm.

DNA Microscopy by Iterative Proximity Ligation (IPL)

Boulgakov and colleagues [26] have recently proposed a DNA microscopy method based on IPL (Figure 2D). Their barcoded molecules are single-stranded oligonucleotides immobilized on a slide surface, corresponding to Figure 1 step 1. This is tantamount to barcoding various locations on the slide. Ligation and restriction are, in principle, reversible reactions (they experimentally confirmed on a population basis that they indeed are). Therefore, it should be possible for the immobilized oligonucleotides to ligate over and over to their various neighbors over multiple rounds of IPL. During each IPL round, incubating the surface with **ligase** would ligate many proximal oligonucleotide pairs throughout the slide. **Primer extending** across the ligated single-stranded pairs would create in solution a new DNA molecule containing both barcodes (i.e., Figure 1 step 2). By incubating the surface with a **restriction enzyme** specific to the ligation site, the oligonucleotides could then revert to their original state. Several such rounds would yield pairwise records for a large proportion of all oligonucleotides. Sequencing the pairs (Figure 1 step 3) would allow a graph to be constructed (Figure 1 step 4), with individual probes as nodes and their ligations as edges. Boulgakov and colleagues have computationally demonstrated that applying a force-directed layout algorithm to such a graph recovers oligonucleotide positions with error on the order of their pairwise lengths (approximately 68 nm), even under suboptimal enzymatic efficiencies (Figure 1 step 5). While this method has not yet been experimentally demonstrated in any robust way, the opportunity to append appropriately encoded DNA molecules to any of a variety of objects, biological or nonbiological, makes it potentially quite generalizable to many applications.

Polony-Based DNA Microscopy (PARSIFT)

Hoffecker and colleagues [27] proposed and simulated a **polony**-based approach to recover molecular positions on a surface (Figure 2E). Primers are arrayed on a surface so as to be able to generate polonies [28] via bridge amplification. DNA seed molecules containing unique barcodes are Poisson deposited onto this surface and then amplified into polonies until they expand to completely tessellate the surface (i.e., Figure 1 step 1). This tessellation is a **Voronoi tessellation** [29].

After tessellation is complete, adjacent DNA strands are randomly crosslinked by depositing bridging oligos (Figure 1 step 2). Extending the bridging oligos captures the barcodes and hence polony identities of adjacent strand pairs (Figure 1 step 3). By representing these observations in a graph-theoretic framework (Figure 1 step 4), with polonies as nodes and adjacencies as edges, with additional constraints provided by properties of the Voronoi tessellation, the authors showed they can recover the spatial positions of the polonies and infer the original positions of the seed molecules (Figure 1 step 5). As a specific demonstration, the authors showed by simulations that they can recover images patterned onto slides, including surprisingly complex examples such as the Mona Lisa.

Error in polony position was evaluated as a fraction of overall image size on the surface and was often below 5% and almost always below 10% of the image radius. Although an absolute distance error was not presented, we can estimate it using some assumptions. We assume that each polony is on the order of 1 μm in diameter and, following the authors, there are 4000 polonies in the image laid out in a circle. This implies that the image radius is approx. 35 μm, so the errors in position are on the order of polony size: often below 1.75 μm and almost always below 3.5 μm. While the proposed method is intellectually interesting, its utility for looking at cells or other biological samples will likely require a method for transferring DNA or RNA from a fixed sample to a surface (any of a variety of tissue print hybridization methods already exist). Alternatively, tagged DNA molecules could be appended to particular features of a surface and the geometry of those features recovered, as described above.

Concluding Remarks and Future Perspectives

The primary driver for all of the technologies listed is their compatibility with NGS, which continues to drive wide swaths of analytical chemistry and biochemistry. DNA microscopy obviates the need for specialized equipment, aside from the now broadly available DNA sequencing platforms; a research facility can tackle many DNA microscopy questions without needing to invest in new equipment for every project [20]. In principle, piggybacking on the exponentially decreasing sequencing costs (https://www.genome.gov/27541954/dna-sequencing-costs-data/) should allow DNA microscopy to observe spatial relationships between billions of components. That said, many development steps remain (see Outstanding Questions), but one example is the delivery of DNA probes into tissue. In cases where the probes are endogenously generated via, for example, transcription, such as in Glaser and colleagues [24] and in the neuron tagging scenario below, this problem does not necessarily arise. However, synthetic probes introduced exogenously face the difficulty of proper distribution in (ostensibly fixed) tissue. The targeting of such probes to specific molecules via, for example, antibodies, is an additional challenge in these scenarios.

Another example is the necessity of space filling so that all local connections can be merged into one whole [20]. Empty spaces that separate islands of DNA-labeled molecules have to be somehow bridged if the islands are to be properly juxtaposed in the broader reconstruction of a whole sample. Furthermore, empty space can significantly distort reconstructions unless we have additional information [26]. Therefore, it is necessary to consider strategies to bridge such gaps, perhaps by complimenting DNA microscopy data with optical imaging or using a 'landmark' approach where we preemptively know the locations of some labels [20]. Once such gaps are breached (metaphorically and physically), the ready availability of NGS allows experiments to be contemplated at scale, meaning that DNA microscopy could potentially multiplex sample imaging to currently unimagined levels.

While only two articles [20,24] explicitly tackle DNA microscopy in three dimensions and the others explore flat surface patterns, the other approaches are not necessarily confined to the

Outstanding Questions

What are the precise trade-offs between sequencing depth and accuracy for the various strategies?

Can we somehow decrease the density of sequences per unit area/volume required by using optical or other 'landmarks' whose positions we obtain from outside (nonsequencing) sources of information, to which the other barcodes can be spatially related?

How can exogenous DNA probes be efficiently delivered into tissue? Is there an upper bound on the volume accessible for the various approaches?

Can DNA microscopy be complemented by tandem use of optical microscopy, for example, by subjecting MERFISH probes to a follow-up round of DNA microscopy that captures labeled proteins or other molecules?

How can we perform microscopy by using noncanonical polymers, such as phosphorothioate DNA which is robust against nucleases, so as to broaden tractable experimental contexts?

How can dynamic information be captured?

plane. The layout algorithm used by Boulgakov and colleagues, for example, is already implemented in software for the 3D case [26]. As their approach substantially resembles that of Schaus and colleagues [21] in the kind of spatial information obtained and in the use of force-directed layout, both are expected to be computationally tractable in three-dimensions.

One tantalizing future application is the spatial mapping of neuron connectivities in the brain [24,30]. Mapping synaptic connections in the brain (the connectome) has been accomplished for *Caenorhabditis elegans* [31,32] and for *Drosophila* using electron microscopy (EM) [33]. In these studies, the sample organism was thinly sliced into layers and each layer was EM imaged at a high resolution, allowing the clearly visible synapse geometries to be reconstructed into models capturing the spatial layout of individual synapse connections. However, EM reconstruction was very painstaking and time-consuming, and such feats will not be accomplished routinely with larger systems such as mice and humans. In contrast, recovering the logical connectome by DNA barcoding neurons and crosslinking these barcodes across synapses is a potentially viable and ultimately scalable approach, and significant progress has already been made towards a proof-of-concept [34–36]. While these strategies share some characteristics with DNA microscopy, mere cellular adjacency does not provide a full picture of neural architecture. Thus, the additional options that DNA microscopy provides for high information content imaging both complement and potentially meld with the connectome approaches that have been pursued.

As a particular example, there is a serendipitous overlap between connectome reconstruction by combining either puzzle imaging or amplicon diffusion DNA microscopies (above) and Peikon and colleagues' neuron barcoding scheme [36]. Peikon and colleagues show that individual neurons can be engineered to express unique mRNA barcodes that localize to synapses and that the barcodes from pre- and post-synaptic neurons can be crosslinked, capturing pairwise synaptic connections as barcode pairs. While this method recovers the logical connectome, it does not provide enough information to reconstruct spatial locales. However, barcoding neurons *à la* Peikon *et al.* and then fixing the brain opens up the possibility that the very same barcodes could be used as a basis for puzzle imaging or amplicon diffusion. For example, *in situ* amplicon diffusion DNA microscopy of a fixed, barcoded brain should in principle recover not only which barcodes are in the same synapse, but also the relative spatial distribution of these synapses. The resolution attained might be further increased by isotropically expanding brain tissues *in situ* with a polymerizing gel before sequencing, yielding the DNA microscopy equivalent of optical expansion microscopy [37–39]. Even further, recent innovations such as molecular ticker tapes that allow events in neurons to be recorded over time might allow DNA microscopy to obtain temporal as well as spatial resolution, leading to a deep understanding of dynamic connectomes [24].

More generally, we can imagine DNA microscopy applications not just for the nervous system, but for tissues in general (e.g., [40]). A prime example would be capturing spatial (re-)organization of cells and tissues during embryonic development or tissue regeneration. As it stands, both developmental and regenerative biology are in the midst of rapid development due to advances in single-cell sequencing technologies. Single-cell RNA-seq can now identify the RNA content of tissues as they develop and, via this RNA content, can also be used to classify individual cells as well as create models of temporal changes in expression and cell types [41–44]. Since changes in expression as cells differentiate from precursors to their final fates are highly consistent between individual cells, it is possible to construct a differentiation 'pseudotime' timeline followed by the entire population and place each individual cell at a different stage along this path (such as in [41,43–45]). DNA microscopy could, in principle, help spatially organize all this information, perhaps even as far as wholesale high-throughput reconstruction of the spatial localization of all transcripts and cell types across entire tissues [24].

References

1. Feynman, R.P. (1992) There's plenty of room at the bottom [data storage]. *J. Microelectromech. Syst.* 1, 60–66
2. Regev, A. *et al.* (2017) The human cell atlas. *eLife* 6, e27041
3. Wang, G. *et al.* (2018) Multiplexed imaging of high-density libraries of RNAs with MERFISH and expansion microscopy. *Sci. Rep.* 8, 4847
4. Lundberg, E. and Borner, G.H.H. (2019) Spatial proteomics: a powerful discovery tool for cell biology. *Nat. Rev. Mol. Cell Biol.* 20, 285–302
5. Gut, G. *et al.* (2018) Multiplexed protein maps link subcellular organization to cellular states. *Science* 361, eaar7042
6. Alber, F. *et al.* (2007) The molecular architecture of the nuclear pore complex. *Nature* 450, 695–701
7. Masters, B.R. (2008) History of the optical microscope in cell biology and medicine. In *Encyclopedia of Life Sciences*, John Wiley & Sons
8. Huang, B. *et al.* (2009) Super-resolution fluorescence microscopy. *Annu. Rev. Biochem.* 78, 993–1016
9. Roy, R. *et al.* (2008) A practical guide to single-molecule FRET. *Nat. Methods* 5, 507–516
10. Nogales, E. and Scheres, S.H.W. (2015) Cryo-EM: a unique tool for the visualization of macromolecular complexity. *Mol. Cell* 58, 677–689
11. Ito, T. *et al.* (2001) A comprehensive two-hybrid analysis to explore the yeast protein interactome. *Proc. Natl. Acad. Sci. U. S. A.* 98, 4569–4574
12. Yu, H. *et al.* (2008) High-quality binary protein interaction map of the yeast interactome network. *Science* 322, 104–110
13. Gavin, A-C. *et al.* (2002) Functional organization of the yeast proteome by systematic analysis of protein complexes. *Nature* 415, 141–147
14. Gao, Q. *et al.* (2014) Chemical inducers of systemic immunity in plants. *J. Exp. Bot.* 65, 1849–1855
15. Stelzl, U. *et al.* (2005) A human protein-protein interaction network: a resource for annotating the proteome. *Cell* 122, 957–968
16. Tarassov, K. *et al.* (2008) An *in vivo* map of the yeast protein interactome. *Science* 320, 1465–1470
17. Havugimana, P.C. *et al.* (2012) A census of human soluble protein complexes. *Cell* 150, 1068–1081
18. Branon, T.C. *et al.* (2018) Efficient proximity labeling in living cells and organisms with TurboID. *Nat. Biotechnol.* 36, 880–887
19. Lam, S.S. *et al.* (2015) Directed evolution of APEX2 for electron microscopy and proximity labeling. *Nat. Methods* 12, 51–54
20. Weinstein, J.A. *et al.* (2018) DNA microscopy: optics-free spatio-genetic imaging by a stand-alone chemical reaction. *bioRxiv* Published online November 19, 2018. https://doi.org/10.1101/471219
21. Schaus, T.E. *et al.* (2017) A DNA nanoscope via auto-cycling proximity recording. *Nat. Commun.* 8, 696
22. Biggs, N. (1993) *Algebraic Graph Theory* (2nd edn), p. 7, Cambridge University Press
23. Kobourov, S.G. (2012) Spring embedders and force directed graph drawing algorithms. Published online January 14, 2012. http://arxiv.org/abs/1201.3011

24. Glaser, J.I. *et al.* (2015) Puzzle imaging: using large-scale dimensionality reduction algorithms for localization. *PLoS One* 10, e0131593
25. Kaufman, A. *et al.* (1993) Volume graphics. *Computer* 26, 51–64
26. Boulgakov, A.A. *et al.* (2018) From space to sequence and back again: iterative DNA proximity ligation and its applications to DNA-based imaging. *bioRxiv* Published online November 14, 2018. https://doi.org/10.1101/470211
27. Hoffecker, I.T. *et al.* (2018) A computational framework for DNA sequencing-based microscopy. *bioRxiv* Published online November 21, 2018. https://doi.org/10.1101/476200
28. Shendure, J. (2005) Accurate multiplex polony sequencing of an evolved bacterial genome. *Science* 309, 1728–1732
29. Aurenhammer, F. (1991) Voronoi diagrams—a survey of a fundamental geometric data structure. *ACM Comput. Surv.* 23, 345–405
30. Zador, A.M. *et al.* (2012) Sequencing the connectome. *PLoS Biol.* 10, e1001411
31. White, J.G. *et al.* (1986) The structure of the nervous system of the nematode *Caenorhabditis elegans*. *Philos. Trans. R. Soc. B Biol. Sci.* 314, 1–340
32. Jarrell, T.A. *et al.* (2012) The connectome of a decision-making neural network. *Science* 337, 437–444
33. Zheng, Z. *et al.* (2018) A complete electron microscopy volume of the brain of adult *Drosophila melanogaster*. *Cell* 174, 730–743
34. Chen, X. *et al.* (2018) High-throughput mapping of long-range neuronal projection using *in situ* sequencing. *bioRxiv* Published online August 31, 2018. https://doi.org/10.1101/294637
35. Han, Y. *et al.* (2018) The logic of single-cell projections from visual cortex. *Nature* 556, 51–56
36. Peikon, I.D. *et al.* (2017) Using high-throughput barcode sequencing to efficiently map connectomes. *Nucleic Acids Res.* 45, e115
37. Chen, F. *et al.* (2015) Expansion microscopy. *Science* 347, 543–548
38. Chen, F. *et al.* (2016) Nanoscale imaging of RNA with expansion microscopy. *Nat. Methods* 13, 679–684
39. Chang, J-B. *et al.* (2017) Iterative expansion microscopy. *Nat. Methods* 14, 593–599
40. Uhlen, M. *et al.* (2010) Towards a knowledge-based human protein atlas. *Nat. Biotechnol.* 28, 1248–1250
41. Rosenberg, A.B. *et al.* (2018) Single-cell profiling of the developing mouse brain and spinal cord with split-pool barcoding. *Science* 360, 176–182
42. Hwang, B. *et al.* (2018) Single-cell RNA sequencing technologies and bioinformatics pipelines. *Exp. Mol. Med.* 50, 96
43. Gerber, T. *et al.* (2018) Single-cell analysis uncovers convergence of cell identities during axolotl limb regeneration. *Science* 362, eaaq0681
44. Plass, M. *et al.* (2018) Cell type atlas and lineage tree of a whole complex animal by single-cell transcriptomics. *Science* 360, eaaq1723
45. Raj, B. *et al.* (2018) Simultaneous single-cell profiling of lineages and cell types in the vertebrate brain. *Nat. Biotechnol.* 36, 442–450
46. Berge, C. (1989) *Hypergraphs: Combinatorics of Finite Sets*, Elsevier